A SILICON MICROVALVE FOR THE PROPORTIONAL CONTROL OF FLUIDS

Kirt R. Williams, Nadim I. Maluf, E. Nelson Fuller, Richard J. Barron,
Dominik P. Jaeggi, and Bert P. van Drieënhuizen

Lucas Varity Corp., Lucas NovaSensor, 1055 Mission Ct., Fremont, California, 94539-8203, USA

ABSTRACT

We present a new type of micromachined plate valve* with pressure-force balancing for operation at elevated pressures. The valve can proportionally control the flow of both gases and liquids. Due to its structure, it can be configured as normally open or normally closed. We have fabricated and tested several versions of the valve, including lower-pressure and higher-pressure valves. The lower-pressure version controls nitrogen up to 1 bar without hysteresis or leakage, and has operated up to 10 bar with a flow rate of 6.7 l/min. The other version controls liquid flow up to 14 bar. The valves are driven by a thermal actuator with a mechanical linkage capable of over 100 μm of motion. The chip is almost entirely silicon, eliminating actuation due to mismatch of thermal expansion rates.

INTRODUCTION

Micromachined Valve Comparison

Most valves use a movable member over an orifice to control the flow of fluid through an orifice [1]. The majority of micromachined valves are seat valves, employing a flexible structure such as a membrane that moves vertically to control the vertical flow of fluid [2,3,4,5]. In contrast, this valve belongs to a family of valves known as sliding plate valves, in which a plate moves horizontally across the vertical flow from an orifice [6]. Plate valves have the advantage over seat valves of being able to, with appropriate design, balance the forces due to pressure in order to minimize the force that must be supplied to the movable member.

Unlike valves that rely on the differential expansion rates of dissimilar materials [2,3,4], this valve uses the temperature difference between heated and unheated structures in single-crystal silicon for actuation. This approach has the advantage of the valve position being relatively unaffected by wide changes in ambient temperature.

Operation

A schematic showing the valve concept, which is implemented in three layers of silicon, is given in Fig. 1. Inlet and outlet ports are formed in top or bottom layers of silicon, or both (these layers are not shown). For the normally open valve shown in Fig. 1, fluid can flow down through an inlet in a top layer of silicon, through the thickness of a second layer of silicon, and continue down out of the outlet.

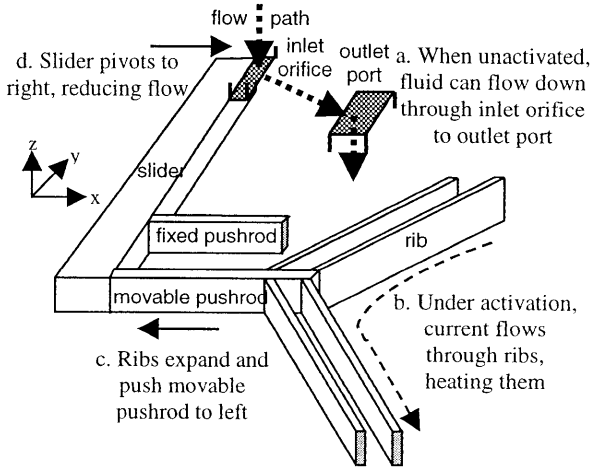

Figure 1 *Schematic of valve concept*

The actuator is formed entirely in the middle silicon layer. The valve is activated by flowing current through the flexible ribs, which heat and expand. The ribs are rigidly held at their ends. The ribs push the movable pushrod to the left in Fig. 1, applying a torque to the slider. The slider tip moves to the right, reducing the orifice area and thus the flow. Fluid is contained in a flow channel by the lower wafer at the bottom, by the middle wafer at the sides, and by the top cap silicon layer. Clearly, many variations on this scheme can be made, including making normally closed valves. Pressure-force-balancing components may be added. The actuator can be designed to consume little power (and operate more slowly), or made for rapid actuation (and higher power consumption).

Because the temperature rise of the ribs relative to the rest of the chip to which the ribs are attached can be continuously varied with input heating power, the slider position over the orifice can be varied, allowing proportional control (i.e., the flow rate varies continuously with input signal [1]).

DESIGN

The valve is comprised almost entirely of single-crystal silicon (SCS), with silicon dioxide used for electrical insulation and metal for bond pads. There

* Patent Pending

are several advantages to using all SCS over other materials or combinations of materials. First, an all-SCS construction is insensitive to fluctuations in ambient temperature. Second, SCS has a high ultimate tensile strength (several times that of polycrystalline silicon) and, unlike metals, does not plastically yield below about 500°C [7]. Third, while thin films are typically limited by practical deposition rates and residual stress to thicknesses of a few micrometers, SCS layers can be made any thickness [13]. High thickness allows the production of very high-output-force (> 1 N) microactuators. Finally, unlike metals, the resistivity of the starting material can be controlled over several orders of magnitude. Thus, the resistance of an actuator of given dimensions can be selected, allowing tailoring of performance specifications of the valve.

Thermal Design

Actuation begins by passing current through the ribs, ohmically heating them. For a given voltage across the ribs, a lower resistance results in higher input power, faster heating, and a higher steady-state temperature profile.

The ends of the ribs are fixed near the temperature of the rest of the chip to which they are attached. The center of each rib pair is the hottest point, with a roughly parabolic temperature profile. Heat is conducted horizontally out the ends of the ribs and also vertically through the dead volume of fluid in which the ribs are suspended. Adjusting the size of the gap between the ribs and the top and bottom layers varies the heat loss and consequently the cooling time and heating power requirement.

After heat is conducted into the main body of the chip, it flows out to the chip surroundings. For a low chip temperature rise, good thermal contact is made to the bottom of the chip. The top of the chip is cooled by the fluid it contacts. When the chip body does heat, it has little effect on the actuator motion because the actuator relies on a temperature *difference* between the chip and the ribs.

Mechanical Design

We choose to use rib pairs [8] as the starting point for actuation because they act linearly rather than in an arc [9,10]. This is useful for driving another stage and allows many pairs to be placed in parallel.

The ribs in these valves are nominally 385 μm thick. Consequently, the forces are much higher than for other micromachined thermal actuators [9,10]. For ribs 100 μm wide, 2000 μm long each, angled at a few degrees, with 10 pairs placed in parallel, for a 100-K average temperature rise, analytical calculations and finite-element simulations show that the force output at the center of the rib pair is about 1.5 N at the start of the stroke. As the ribs move, the force output falls nearly linearly to zero at the end of the stroke, which is about 7.5 μm in this example.

For the present valve application, this large force and relatively small displacement are transformed into a larger displacement using a lever. Rather than using a mechanical pivot point, which would be difficult to fabricate and could pose reliability problems from parts grinding against each other, we choose a flexure structure, as shown in Fig. 1. The fixed pushrod serves as the pivot point. After accounting for loss in the pushrods, the unloaded x slider-tip displacement is approximately equal to the lever ratio (the slider length measured from the fixed pushrod divided by the pushrod spacing) times the rib displacement.

Flow Design

Flow enters the chip from the top port and leaves through the bottom port. This has the advantages of allowing simple packaging in a can such as a modified TO-8 header with tubes (Fig. 2). In such an arrangement, the chip and adhesive layer are in compression when pressurized, reducing the demands on the bonding between the silicon layers and of the chip to the package. A disadvantage is that the electrical contacts on the top of the chip are in contact with the fluid.

In micromachined seat valves, the membrane must work against the force of a pressure difference acting over the orifice area. This limits the maximum operating pressure. In the plate valve design, however, the static pressure forces can be balanced (Fig. 3). We have accomplished balancing by adding an open silicon rectangle to the slider end so that the inlet pressure p_{in} acts against opposing surfaces of the rectangle in the x and y directions. The outlet pressure is allowed to surround the outside of the rectangle so that it, too, acts on opposing surfaces.

The slider is also pressure-force-balanced in the vertical (z) direction by the formation of a cavity under the leading edge of the slider. This also allows flow from both sides of the slider. Without this

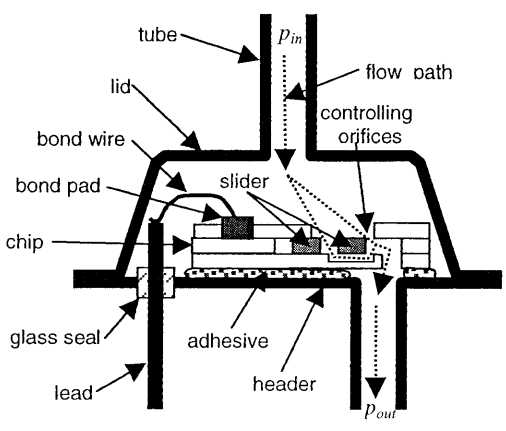

Figure 2 *Cross section of valve in package*

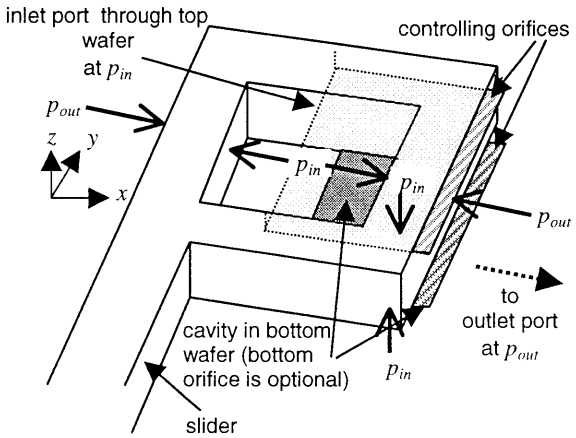

***Figure 3** Pressure-force balancing*

balancing, experiments show that the friction due to the force pushing down on the slider limits operation to low pressures.

Port Sizing

The volumetric flow rate Q through an orifice for an incompressible fluid is determined primarily by the pressure drop $\Delta p = p_{in} - p_{out}$, the total orifice area A, and the fluid density ρ. The flow rate is also affected to a small degree by the shape of the orifice, the amount of flow convergence just after exiting the orifice (the *vena contracta*), and the Reynolds number [1,11]. These effects are taken into account in the empirical unitless discharge coefficient C_D (with typical values of 0.6-0.7 [12]) in the equation

$$Q = C_D A\sqrt{2\Delta p / \rho} \quad . \qquad (1)$$

The pressure drop in Eq. 1 is across the orifice and does not take into account viscous losses in the fluid routing entering and exiting the orifice. Computational fluid dynamics modeling using software supplied by CFDRC (Huntsville, Alabama) shows that these losses are small for the valve structures presented here.

FABRICATION

The valve fabrication process flow is shown schematically in Fig. 4. The top and bottom silicon layers are to a large degree mirror images of each other. Processing of the top and bottom wafers starts with the etching of shallow cavities over and under the future locations of all moving parts. This depth sets the gap for the fluid leakage path past the slider when the valve is closed. Subsequent etching steps form deep thermal isolation trenches above and below the ribs in low-power valves. The unpatterned middle wafer is silicon fusion bonded (SFB) to the bottom wafer. A double-sided alignment and deep reactive ion etch (DRIE) form the freed actuator in the middle wafer [8,13]. Aligned SFB adds the top wafer to the stack. Finally the wafer is metallized to form contacts. A die photograph of the valve is

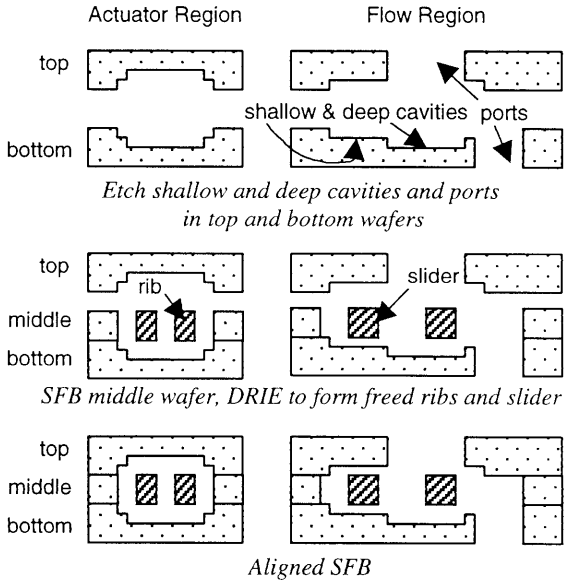

***Figure 4** Fabrication process flow*

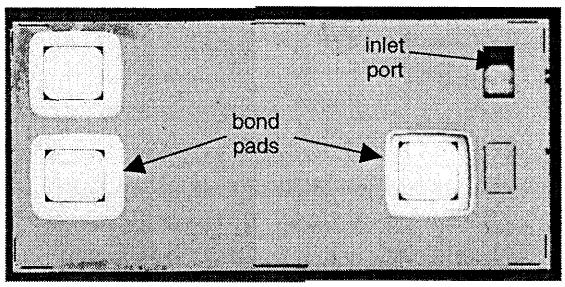

***Figure 5** Die photograph of valve*

shown in Fig. 5.

The valves are packaged in a modified TO-8 header with inlet and outlet tubes in the lid and base. The chips are adhered with RTV adhesive. After wire bonding, the lid is resistively welded on.

TEST

Figure 6 is a sequence of three photographs of a two-layer prototype valve showing the variable orifice opening that allows proportional control of fluid flow. The slider moves over 100 μm.

For the lower-pressure valves, the room-temperature actuator resistance is 187 Ω. Applying a voltage of 20

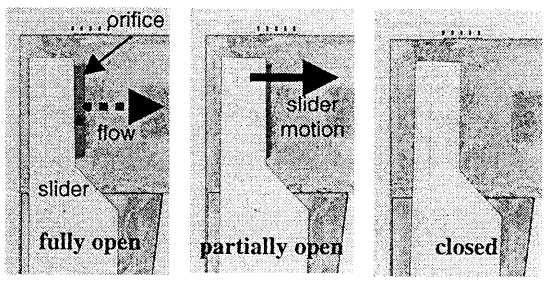

***Figure 6** Variable orifice opening for proportional control*

V heats the ribs to an average temperature of 100 K above room temperature, increasing the resistance to 292 Ω and yielding a heating power of about 1.4 W. The chip temperature, monitored with an on-chip reference resistor, rises about 45 K in steady state.

Flow-rate data for nitrogen (measured at atmospheric pressure) as a function of power is presented in Fig. 7 for a normally open (N/O) valve with both upper and lower orifices and in Fig. 8 for a normally closed (N/C) valve with only an upper orifice (*cf.* Fig 3). Below 1 bar (10^5 Pa), there is negligible hysteresis as the N/O valve is activated and deactivated. Hysteresis is seen for the N/C valve due to its lack of *z*-axis pressure-force balancing. Both valves show leakages below 0.2 ml/min (the flowmeter resolution). Figure 9 shows data for pressures up to 10 bar for the N/O valve. We have observed hysteresis and leakage at higher pressures, indicating imperfect force balancing and closure.

A higher-pressure normally closed valve has been used to control liquid at a pressure of 13 bar and flow rates up to 300 ml/min.

The response time of the valves is less than 0.5 s, measured by observing the flowmeter for step changes in input pressure.

ACKNOWLEDGMENTS

We thank I. Taher, R. Scimeca, S. Wong, C. Darnell, A. Kollipara, and C. Lowman for their assistance.

REFERENCES

[1] D. McCloy and H. R. Martin, *Control of Fluid Power: Analysis and Design, 2nd Ed.*, Chichester, Ellis Horwood Ltd., 1980, Chs. 4 and 6

[2] A. K. Henning, J. Fitch, D. Hopkins, L. Lilly, R. Faeth, E. Falsken, and M. Zdeblick, "A Thermopneumatically Actuated Microvalve for Liquid Expansion and Proportional Control" Proc. Conf. Solid State Sensors and Actuators (Transducers '97), Chicago, Illinois, USA, Jun. 16-19, 1997, pp. 825-828

[3] X. Wang, C. Grosjean, and Y.-C. Tai, "A Low Power MEMS Silicone/Parylene Check Valve" Proc. Solid-State Sensor and Actuator Workshop (Hilton Head '98), Hilton Head Island, South Carolina, USA, June 8-11, 1998, pp. 316-319

[4] J. Haji-Babaei, C. Y. Kwok, and R. S. Huang, "Integrable Active Microvalve with Surface Micromachined Curled-Up Actuator" Proc. Conf. Solid State Sensors and Actuators, Chicago, Illinois, USA, pp. 833-836

[5] A. Meckes, et al., "Electromagnetically Driven Microvalve Fabricated in Silicon" Proc. Conf. Solid State Sensors and Actuators, Chicago, Illinois, USA, Jun. 16-19, 1997, pp. 821-824.

[6] M. Walters, V. Dhuler, R. Mahadevan, A. Cowen, R. Wood, E. Hill, and I. Kao, et al., "A Silicon Micromachined Gate Valve," Proc. Solid-State Sensor and Actuator Workshop, Hilton Head Island, South Carolina, USA, June 8-11, 1998, Late News pp. 27-28

[7] C. Keller, *Microfabricated High Aspect Ratio Silicon Flexures*, El Cerrito, MEMS Precision Instruments, 1998, Sec. 1.1.3

[8] E. Klassen, K. Petersen, J. M. Noworolski, J. Logan, N. Maluf, J. Brown, C. Storment, W. McCulley, and G. T. A. Kovacs, "Silicon Fusion Bonding and Deep Reactive Ion Etching: A New Technology for Microstructures" Proc. Conf. Solid State Sensors and Actuators, June 25-29, 1995, Stockholm, Sweden, pp. 556-559

[9] J. H. Comtois and V. M. Bright, "Surface Micromachined Polysilicon Thermal Actuator Arrays and Applications" Proc. Solid-State Sensor and Actuator Workshop, Hilton Head Island, South Carolina, USA, June 3-6, 1996, pp. 174-177

[10] P. B. Allen, J. T. Howard, E. S. Kolesar, and J. M. Wilken, "Design, Finite Element Analysis, and Experimental Performance Evaluation of a Thermally-Actuated Beam Used to Achieve Large In-Plane Mechanical Deflections" Proc. Solid-State Sensor and Actuator Workshop, Hilton Head Island, South Carolina, USA, June 8-11, 1998, Late News pp. 5-6

[11] R. W. Fox and A. T. McDonald, *Introduction to Fluid Mechanics, 4th Ed.*, New York, Wiley, 1992, Sec. 8-10

[12] J. F. Blackburn in *Fluid Power Control*, J. F. Blackburn, G. Reethof, and J. L. Shearer, eds., New York, Wiley, 1960, Ch. 7

[13] K. R. Williams, "New Technology and Applications at Lucas NovaSensor," in *Tribology Issues and Opportunities in MEMS*," Bharat Bhushan, ed., Dordrecht, Kluwer, 1997, pp. 121-134

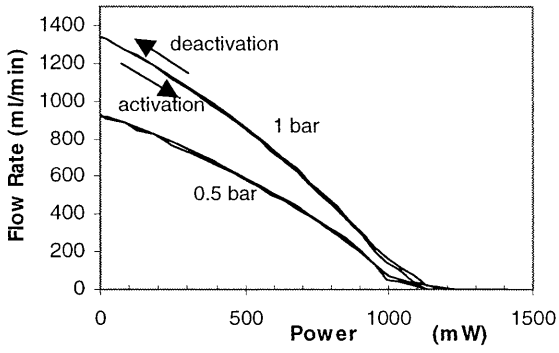

***Figure 7** Flow rate of N_2 vs. power and pressure for a two-orifice normally open valve*

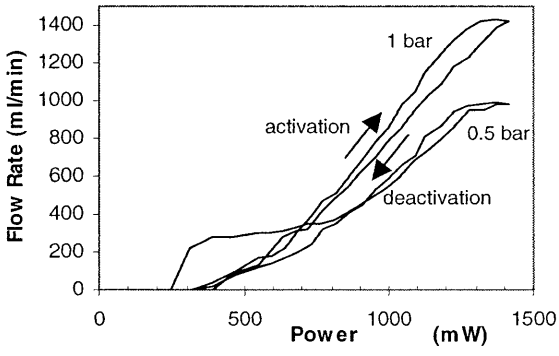

***Figure 8** Flow rate of N_2 vs. power and pressure for a one-orifice normally closed valve*

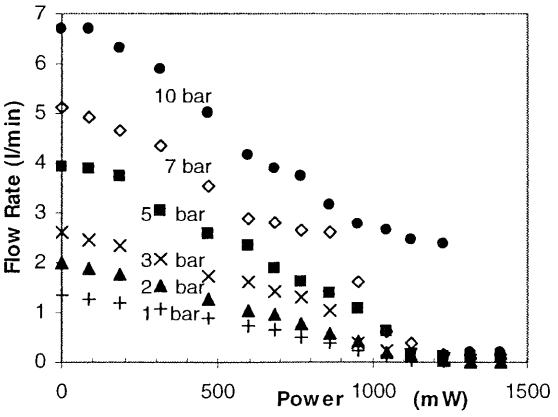

***Figure 9** Flow rate of N_2 vs. power up to 10 bar*